

A model of time estimation and error feedback in predictive timing behavior

Wilsaan M. Joiner · Mark Shelhamer

Received: 20 December 2007 / Revised: 16 April 2008 / Accepted: 16 May 2008 / Published online: 19 June 2008
© Springer Science + Business Media, LLC 2008

Abstract Two key features of sensorimotor prediction are preprogramming and adjusting of performance based on previous experience. Oculomotor tracking of alternating visual targets provides a simple paradigm to study this behavior in the motor system; subjects make predictive eye movements (saccades) at fast target pacing rates (>0.5 Hz). In addition, the initiation errors (latencies) during predictive tracking are correlated over a small temporal window (*correlation window*) suggesting that tracking performance within this time range is used in the feedback process of the timing behavior. In this paper, we propose a closed-loop model of this predictive timing. In this model, the timing between movements is based on an internal estimation of stimulus timing (an internal clock), which is represented by a (noisy) signal integrated to a threshold. The threshold of the integrate-to-fire mechanism is determined by the timing between movements made within the correlation window of previous performance and adjusted by feedback of recent and projected initiation error. The correlation window size

increases with repeated tracking and was estimated by two independent experiments. We apply the model to several experimental paradigms and show that it produces data specific to predictive tracking: a gradual shift from reaction to prediction on initial tracking, phase transition and hysteresis as pacing frequency changes, scalar property, continuation of predictive tracking despite perturbations, and intertrial correlations of a specific form. These results suggest that the process underlying repetitive predictive motor timing is adjusted by the performance and the corresponding errors accrued over a limited time range and that this range increases with continued confidence in previous performance.

Keywords Prediction · Saccade · Timing · Error feedback

1 Introduction

Saccades are fast conjugate changes of eye position between fixations, such as are made when reading this sentence. The predictive saccade task typically requires a subject to track a visual target that alternates between two fixed positions at a fixed rate or interstimulus interval (ISI; see Fig. 1(a)). In other words, both the temporal and spatial properties of the stimulus remain constant throughout the test session and therefore are completely predictable. A number of investigators have used variations of this paradigm to study predictive capabilities in both normal human subjects (Stark et al. 1962; Ross and Ross 1987; Zambardi et al. 1987; Shelhamer and Joiner 2003; Isotalo et al. 2005; Shelhamer 2005; Joiner and Shelhamer 2006a, b; Zorn et al. 2007) and in patients with neurological disease (Bronstein and Kennard 1984, 1985; Tian et al. 1991; Ventre et al. 1992;

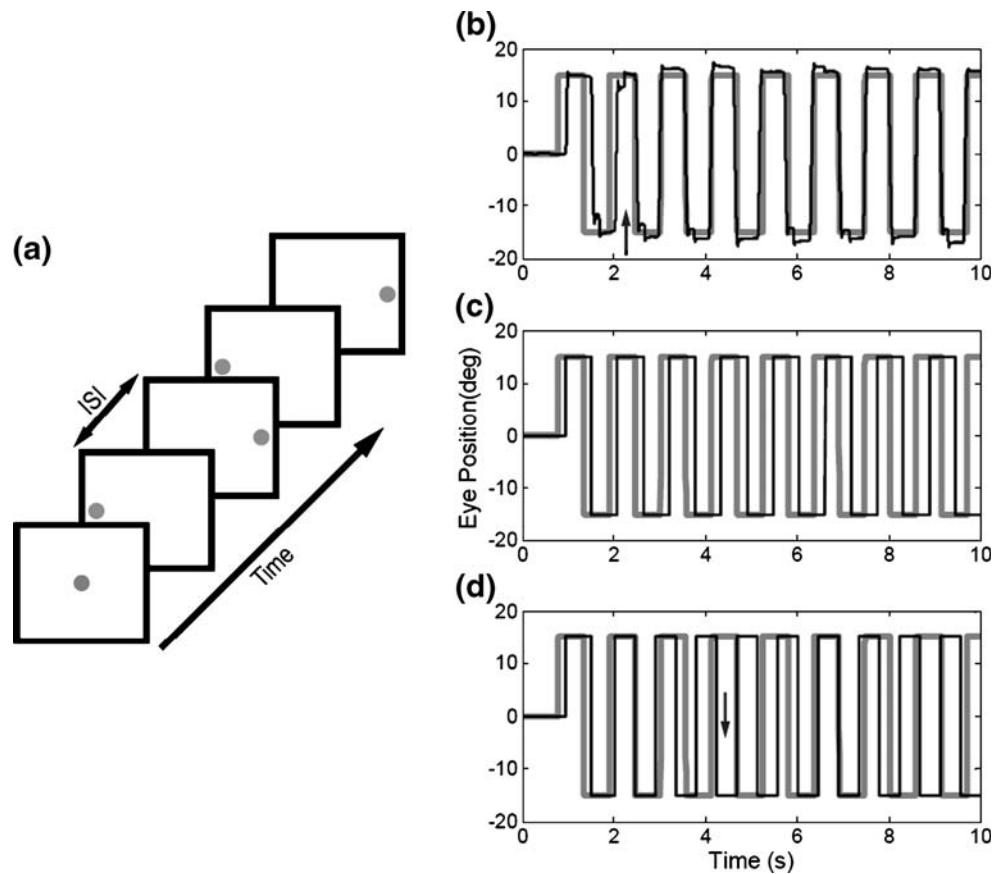
Action Editor: Matthew Wiener

W. M. Joiner
Laboratory of Sensorimotor Research, National Eye Institute,
National Institutes of Health,
Bethesda, MD 20892, USA

M. Shelhamer
Department of Otolaryngology—Head and Neck Surgery,
Department of Biomedical Engineering, School of Medicine,
The Johns Hopkins University,
Baltimore, MD 21287, USA

W. M. Joiner (✉)
Laboratory of Sensorimotor Research,
National Institutes of Health,
49 Convent Drive,
Bethesda, MD 20892, USA
e-mail: joinerw@nei.nih.gov

Fig. 1 (a) Diagram of the predictive-saccade task. The gray circle represents the target which at the start of the experimental session begins at midline (*first panel*) and then alternates between two fixed positions at a fixed rate (interstimulus interval, *ISI*). (b) Behavioral results for one subject during the predictive-saccade task. The black trace represents the eye movement; the gray trace is target position. (c) Simulated results not using feedback of intersaccade intervals. (d) Simulated results not using feedback of timing errors (latency)



Krebs et al. 2001). More recently, functional imaging of the brain has been used to investigate the neurological areas responsible for this ability (Gagnon et al. 2002; Simó et al. 2005; Burke and Barnes 2008).

Predictive tracking of alternating targets requires the correct movement timing (an intersaccade interval close to the ISI) and the appropriate movement latency (less than the time required for a typical saccadic eye movement, approximately 80 ms; Zorn et al. 2007). A sequence of predictive saccades from a typical normal subject in this paradigm is displayed in Fig. 1(b). Target position is represented by the gray line; the black line represents the subject's eye position. As displayed in the figure, when the subject begins to track the alternating targets the first two saccades are reactive (they occur after the stimulus jump with respective latencies of 161 and 166 ms). This is due to the subject having no prior knowledge of the stimulus timing. However, by the fourth saccade, the eye movement occurs with a latency of 12 ms signifying that it is a preplanned predictive movement (visual processing and motor delay require approximately 80 ms). This predictive tracking behavior utilizes two sources of feedback from previous movements: the timing between movements (intersaccade interval) and the timing error (latency). Initially, to overcome the early timing error (the reactive latencies of 161 and 166 ms), the subject must decrease the

intersaccade interval as marked by the upward arrow in panel (b). Then, following this adjustment, the subject tracks the targets with minimal timing error: The subject's eye movements are in phase with the stimulus. The intersaccade intervals and latency values of the subsequent saccades are approximately 556 (the same as the timing of the stimulus: the ISI) and near 0 ms, respectively.

This adjustment and subsequent tracking behavior is not a trivial phenomenon. For example, if the subject continued to make saccades with the same timing as the first intersaccade interval (that is, no adjustments to the time between saccades), then subsequent saccades would never become predictive, and the error would continue to increase with each eye movement. This is simulated in Fig. 1(c); note that the eye and target (black and gray traces) become more out of phase with each eye movement. In addition to making adjustments based on the timing between previous movements, the subject must also take the latency or initiation error of previous saccades into account. For example, if the subject adjusts the intersaccade interval as in panel (b) but makes no further adjustments (i.e., maintains this new intersaccade interval), then subsequent eye movements will be predictive (occur before the corresponding stimulus jump), but the timing error will increase substantially with each movement. This is simulated in Fig. 1(d). In this case, the subsequent saccades are

predictive, but the movements are out of phase with the stimulus as marked by the downward arrow in panel (d). Thus, predictive tracking of alternating targets involves adjustments based on both previous intersaccade intervals and latency values (Zorn et al. 2007).

There are three behavioral results found recently in our laboratory that suggest that the predictive tracking behavior displayed in Fig. 1(b) is based on the internal representation of target timing (i.e., an internal clock), which is modified by the two sources of feedback discussed above. We now review these three behavioral results, as they are relevant to the proposed model that is the main outcome of this study.

1.1 Continuation of timing despite perturbations

The first relevant behavioral result is the continuation of predictive saccade timing despite transient changes to the timing of the stimulus. For example, when the ISI suddenly changes from small to large (500 to 2500 ms, which is an abrupt stimulus pacing change from fast to slow) after a period of steady-state tracking, subjects continue to make eye movements at the faster pacing rate, although the target pacing has changed (Joiner and Shelhamer 2006a; Joiner et al. 2007a). As shown in Fig. 2(a), the subject makes saccades (black line) with intervals of approximately 500 ms (the eye movements made within the black dashed line box) after the stimulus pacing perturbation (gray line). This is also the case if the targets are suddenly extinguished. As depicted in Fig. 2(b), after the targets are

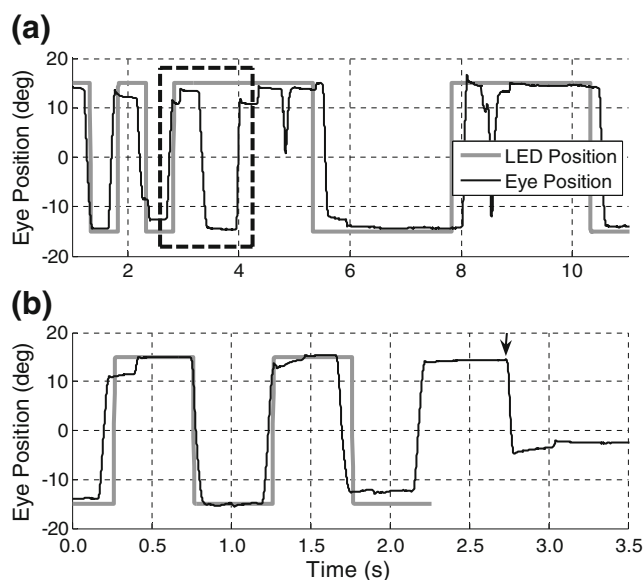


Fig. 2 Behavioral results supporting an internal clock in the generation of predictive saccades. Following steady-state predictive tracking, the subject (*black trace*) continues to track at this rate despite (a) abruptly increasing the ISI or (b) extinguishing the targets (*gray trace*). With kind permission of Springer Science+Business Media

abruptly turned off (end of the gray line), the subject makes one additional internally triggered saccade without a visual stimulus (marked by the downward arrow) with an interval of approximately 500 ms (typically, subjects will make two to three such saccades; see Joiner and Shelhamer 2006a; Shelhamer 2005). The finding that steady-state predictive tracking continues in complete darkness and in spite of changes to the stimulus timing demonstrates that the required eye movement timing is stored in neural memory and thus the timing behavior is partly independent of the stimulus.

1.2 Correlation window

The second result is the finding of correlations between successive predictive saccades: The autocorrelation function of the latency time series (consecutive latency values) during predictive saccade tracking decays slowly, whereas the autocorrelation for reactive tracking decays very quickly with increasing intertrial interval (Shelhamer and Joiner 2003). In other words, the latencies of eye movements separated by several trials during predictive tracking are correlated (see Fig. 3(d)), while those of reactive saccades are largely independent. The slow decay for predictive tracking indicates that there is “significant” correlation between saccade latencies and suggests that current movements are based upon (due to the feedback) prior movements occurring earlier in the time series. A study of this phenomenon (Shelhamer 2005) analyzed the slow decay of the autocorrelation function to estimate the “correlation window” over which subjects utilized this feedback at different pacing rates. That study showed that sequences of predictive saccades made at different pacing rates are correlated over a window of approximately 2 s (initially when tracking begins). A related observation is that the ability to synchronize with a pacing stimulus at ISIs larger than 2 s breaks down for both repetitive tapping (MacDorman 1962; Mates et al. 1994; Miyake et al. 2004) and saccadic eye movement tracking (Stark et al. 1962; Ross and Ross 1987; Shelhamer and Joiner 2003; Joiner and Shelhamer 2006a, b). These and other results (Getty 1975; Chen et al. 2002) suggest that the influence of feedback occurs within this 2-s time span of previous movements.

Another observation regarding the autocorrelation function of the predictive latency time series is that as predictive tracking continues for many trials (approximately 1,000 trials), the correlation window gradually increases. We made this observation initially in our previous work (Shelhamer 2005) and verify and quantify it here experimentally (described below). The basic finding is that as subjects track for extended durations, they incorporated performance further in the past into their

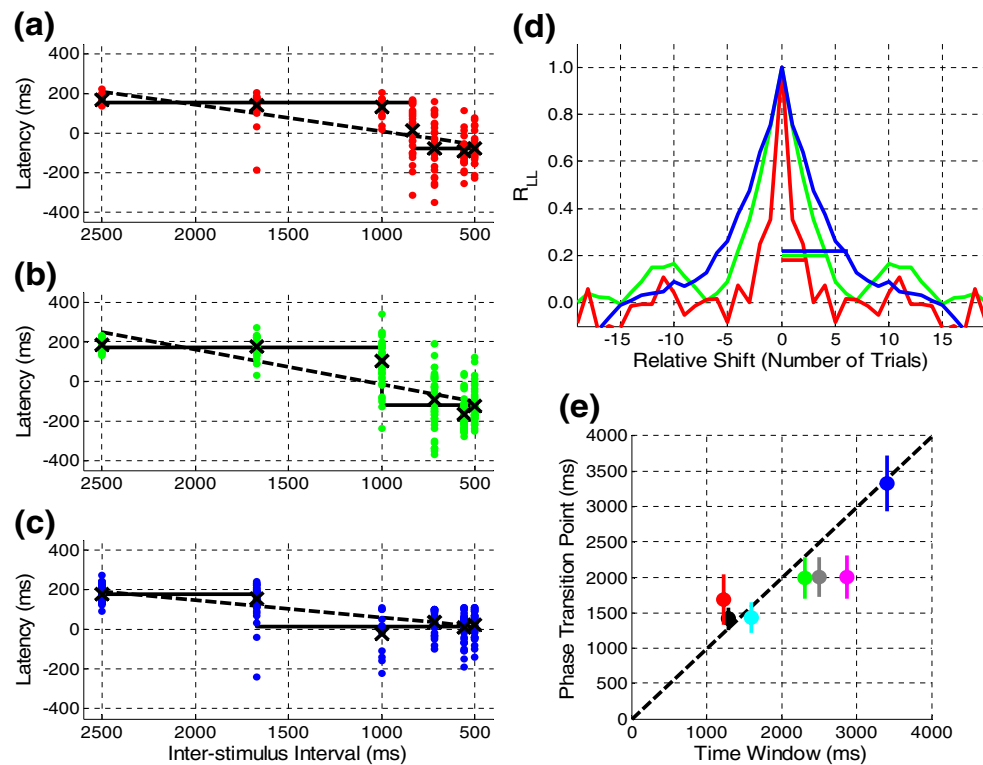


Fig. 3 (a, b, c) Three subjects that exhibit the behavioral transition in tracking behavior (phase-transition experiment) as ISI monotonically decreases. The *circles* in each panel represent the saccade latency for a single trial (target jump). The *thick black X* is the average saccade latency for a given ISI. The *solid* and *dashed black lines* represent an abrupt transition fit and a linear regression fit to the data, respectively. As demonstrated in each panel, saccade latency makes a rapid transition from reactive to predictive as ISI decreases. The critical ISI at which the transition occurs is different for each subject; (a) 833, (b) 1,000 ms, and (c) 1,667 ms. (d) Autocorrelation functions

determined from the latency series at 0.9-Hz pacing (approximately 300 trials) for the same three subjects presented in (a), (b), and (c). Latency autocorrelation functions also result in different correlation window lengths (determined when the function crosses a threshold of 0.2, represented by the *horizontal bars*) for the three subjects. (e) The critical ISI for the phase-transition experiment (*ordinate*) scales with the correlation-window length estimated from the autocorrelation functions (*abscissa*) for seven subjects, demonstrating a correspondence between the two

predictions: They build up a statistical model of confidence in the stimulus. This is revealed by an increase in the width of the autocorrelation function with trial number and gives rise to hysteresis in the transition between reactive and predictive tracking, as we show below.

1.3 Scalar property

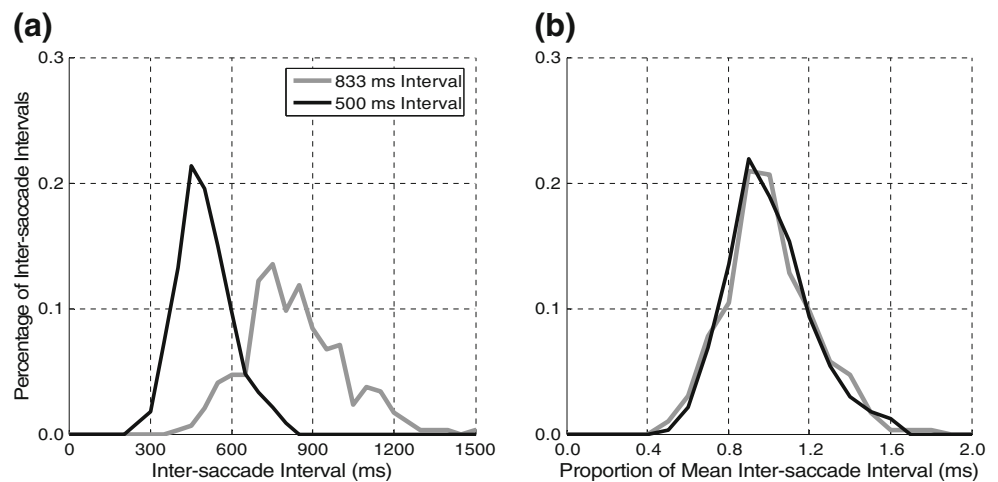
The third pertinent result is that distributions of intersaccade intervals for predictive tracking at different pacing rates demonstrate the scalar property. As shown by others (Gibbon 1977; Gibbon et al. 1997; Medina et al. 2005), when making movements based on an internal estimate of stimulus timing, the standard deviation of the intermovement interval distribution is proportional to the interval length. This is evident during predictive tracking at different ISIs; the larger the ISI, the more variability in the intersaccade interval distribution (Fig. 4(a) but also see Joiner and Shelhamer 2006a; Joiner et al. 2007b). Furthermore, if response timing during the interval timing

task is the result of an internal timing process, then the response time interval distributions will be approximately identical when scaled by the mean of each distribution, a result known as the scalar property (Gibbon 1977; Gibbon et al. 1997; Buhusi and Meck 2005). The timing of saccades during predictive tracking readily demonstrates this property; the intersaccade interval distributions from two different ISIs (500 and 833 ms, Fig. 4(a)) overlap when each distribution is normalized by its corresponding mean interval (Fig. 4(b); Joiner and Shelhamer 2006a, Joiner et al. 2007b). Reactive tracking does not exhibit this property.

1.4 Internal clock model

The established framework for describing interval timing and the scalar property is an internal clock model (Treisman 1963; Gibbon 1977; Meck and Benson 2002). The first stage of this model is the estimation of time, which is accomplished by the neural accumulation of pulses emitted

Fig. 4 Behavioral results demonstrating the scalar property. **(a)** Distributions of intersaccade intervals at predictive pacing rates (ISIs of 833 and 500 ms) vary around the ISI, and the variability increases with interval length. **(b)** When these distributions are divided by the mean interval, they overlap, demonstrating the scalar property. With kind permission of Springer Science+Business Media



by a pacemaker (Woodrow 1930; Hoagland 1933; the pulses have recently been hypothesized to be the action potentials emitted by dopaminergic neurons in the basal ganglia, see Matell and Meck 2004). Once the accumulation of the pulses stops, the accumulated value is compared with a sample value of the expected number of pulses (representing the required time duration) stored in memory. If the accumulated value is within the range of the value in memory, a response is made (for example, an eye or hand movement). The accumulated value, representing the most recent inter-response interval, is then pooled with the distribution of samples stored in memory. In this way, the new value stored in memory can affect subsequent timing behavior through feedback of past performance. Rather than the accumulation of pulses, this process can also be described as the integration, over time, of some noisy signal representing the rate of an internal counter. When the integrated signal reaches a threshold, a timed event occurs (a movement), and the integrator is reset to start a new cycle. The error between the time that the integrated signal reached threshold and the desired time interval as determined by an external stimulus can then be used to adjust the timing of future movements via changes in the integration threshold (feedback). The integrated signal has a random component due to neural noise, and this leads to randomness in the event times. More specifically, the longer the interevent interval, the longer is the integration time of the random signal, and hence the more variability there will be in the event times (Schöner 2002). In this framework, the scalar property derives naturally from the fact that the variability of estimating the passage of time is proportional to the interval being estimated (Buhusi and Meck 2005).

Despite the success of internal clock models in explaining a large set of behavioral and physiological results (Buhusi and Meck 2005), established *clock* models of repetitive movements do not include the

feedback described above. For example, one of the first motor-timing models for repetitive tapping to a pacing metronome (Wing and Kristofferson 1973a, b) incorporated a clock mechanism in the timing of movements (in these repetitive tapping experiments, subjects are required to tap their index finger in synchrony with a pacing metronome). This model separated total timing error into central clock variance and motor delays and assumed that clock intervals and motor delays were independent from trial to trial. This results in a negative dependence between successive intervals (short intertap intervals are likely to be followed by large intertap intervals and vice versa), with no correlation beyond that. As previously shown (Shelhamer and Joiner 2003; Shelhamer 2005), this short-term negative correlation does not hold for sequences of predictive saccades, which exhibit extensive long-term correlations between movements. This and other results (Collins et al. 1998) confirm that repetitive predictive tracking is not an open-loop process and must depend on some source of feedback.

Other nonclock models of repetitive tapping incorporate various forms of feedback in interval production. Michon (1967) proposed a “linear predictor model” in which feedback is restricted to the immediately preceding interval but lacks any correction based on synchronization error (tapping latency). Hary and Moore (1985, 1987a, b) suggested a mixed reset model in which feedback is restricted to the synchronization error of the previous two movements. Similar to the simulation shown above in Fig. 1(c), these authors showed that without such feedback control, the metronome and the tapping responses of the subject will become out of phase due to the variability of the tapping responses (Hary and Moore 1987b). In addition to this feedback, the model incorporates a random switching between two resetting strategies: *metronome reset* in which the next interval is timed from the previous metronome event and *response reset* in which the next

interval is timed from the previous tapping response (Schulze 1992). The second resetting strategy will be discussed in more detail in Section 2. Similar to Hary and Moore, Vorberg and Wing (1996) also proposed a model in which synchronization error was the only source of feedback. More recent models (Vos and Helsen 1992; Mates 1994a, b) include the feedback of both synchronization errors and inter-response intervals but only utilize a fixed number of previous responses. As a result, these models do not sufficiently reproduce the behavioral results described above for repetitive predictive saccades (e.g., long-term correlations between synchronization errors).

There has been one previous model of predictive saccade tracking of targets that alternate in either a symmetric or asymmetric square wave pattern (Schmid and Ron 1986; Ron et al. 1989). The model assumed a predictor in each cerebral hemisphere and was developed using steady-state tracking data (disregarding the first five cycles of the stimulus). By basing the model on this limited data, predictive tracking was not formulated as the result of feedback from the sources previously described for Fig. 1(b)–(d). In addition, the prediction of the targets was not due to an internal timing storage as demonstrated in Fig. 2(a) and (b). Rather, the ability to predict (the simulated response time of the eye movement) was based on excitation and inhibition signals (within each hemisphere) whose accumulation and decay rates were dependent upon the stimulus timing (cycle duration) and the degree of asymmetry of the square wave pattern. This is an oversimplified depiction of the tracking behavior that the authors themselves conceded in their discussion: “This model can therefore be proposed as the simplest way to interpret the general behavior of a subject tracking with his eyes a symmetrical or asymmetrical square wave pattern of target motion.”

Our goal was to develop an accurate model of the behavior exhibited during predictive saccade tracking that utilizes a combination of the concepts previously described: (1) reproducing predictive tracking as the outcome of an internal clock (estimating the time between movements based on an internal timing storage), (2) utilizing feedback of previous intersaccade intervals and timing error/latency, and (3) incorporating a time span of past movements over which this feedback is acquired (a *correlation window*). The model we describe here reproduces the behavioral results described above: (1) the continuation of predictive saccade tracking despite perturbations to the stimulus, (2) the demonstration of the scalar property by the intersaccade intervals during predictive saccade tracking, (3) the long-term correlations between predictive tracking synchronization errors, and also (4) the behavioral phase transition and hysteresis in

tracking behavior (reactive to predictive and vice versa), which is described in Section 2.

2 Materials and methods

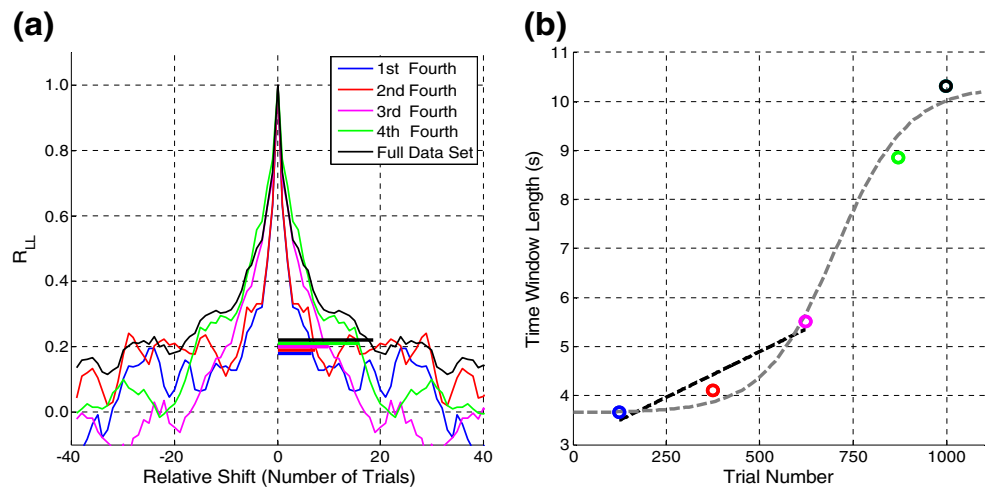
This section is divided into three parts. First we describe the experimental setup and procedure used to obtain the previously published behavioral results (presented in Figs. 1, 2, 3, 4, 6, 8, and 10, 11, 12) and a recent experiment used to determine the rate of growth of the correlation window as a function of extended predictive tracking (Fig. 5). Next, we describe the formulation of the timing model. Finally, in the third section, we describe a second experiment (the phase-transition experiment) and the estimation of model parameters from these behavioral results.

2.1 Experimental setup and procedure

The experimental data presented in Figs. 1, 2, 3, 4, 6, 8, and 10, 11, 12 was obtained from eight subjects while they performed different eye movement tasks (for details, see Shelhamer and Joiner 2003; Shelhamer 2005; Joiner and Shelhamer 2006a, b; Joiner et al. 2007a, b). Informed consent, according to the local institutional research board, was obtained from each participant. Eye movement data were acquired on a personal computer-compatible Pentium 166-MHz computer running real-time experiment control software developed in-house. Horizontal movements of the eyes were recorded with a Series 1000 Binocular Infrared Recording System (Microguide), sampled at 1,000 Hz. The system was calibrated prior to data acquisition by having subjects fixate visual targets at known locations. Subjects were seated in a dark room in a stationary chair in front of a tangent screen (124 cm in front of the subject) on which were located two light-emitting diode targets (3 mcd) on either side of the vertical midline (left and right 15°). The head was fixed with a chin rest. Subjects were given no explicit instructions as to timing or accuracy; they were told simply to “look at the target.”

Analysis of eye-tracking data was done offline. First, eye velocity was calculated using a four-point digital differentiator based upon a least-squares derivative algorithm (Savitzky and Golay 1964). This is an efficient iterative method of fitting a third-order polynomial to each data point and the preceding and following two values, then finding the derivative of the fitted polynomial. Eye movement latency was determined by comparing the onset of the primary saccade to the onset of the target in each trial. Saccade onset was determined using a velocity threshold ($\geq 60^\circ/\text{s}$).

Fig. 5 (a) Autocorrelation functions for one subject (approximately 1,000 trials) for different data segments. The data series was divided into four segments of approximately 250 trials each. These segments resulted in different correlation window lengths. (b) Correlation window lengths for the five autocorrelation functions presented in (a). The black dashed line is a linear fit to the first three segments (as used in the model). The gray dashed line is a logistic function fit to all segments



The intersaccade interval was the time between each primary saccade.

2.2 Experiment: extended tracking

We wished to confirm our initial findings on the size of the correlation window as a function of number of predictive saccades (Shelhamer 2005). Five subjects (one example depicted in Fig. 5) made 1,000 consecutive saccades at the predictive pacing rate of 0.9 Hz (ISI of 556 ms). The series of latency values was divided into four 250-point nonoverlapping segments. The autocorrelation function of each segment was found, and the size of the correlation window in each case was determined as the half-width (since it is symmetric) of the autocorrelation function at a correlation

value of 0.2, as in our previous studies (Shelhamer 2005; Joiner and Shelhamer 2006c).

2.3 Model construction

To simulate predictive tracking of alternating targets, we have constructed a closed-loop model that (1) builds an internal estimation of the stimulus timing based on previous intermovement intervals and (2) adjusts this time estimate through the feedback of the preceding initiation error and the projected initiation error of the time estimate. The model can be used to examine both the short-term (perturbations to the stimulus timing) and long-term (scalar property of intersaccade intervals) behaviors of the timing system.

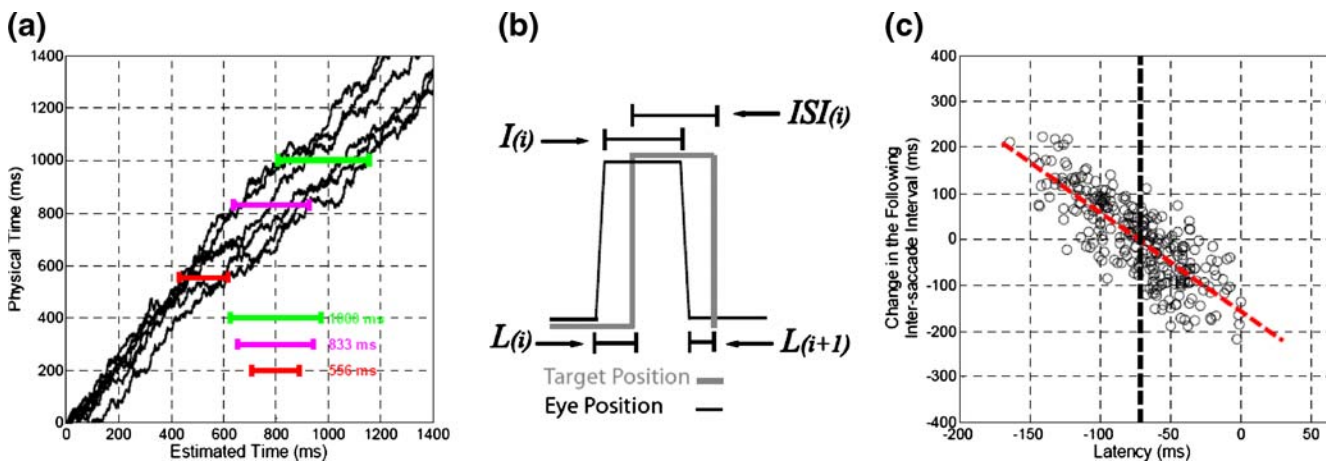


Fig. 6 (a) Time estimation is modeled as the accumulation of a noisy signal to a threshold. Five example time estimation signals are shown. Variability of the physical time estimate (crossing of the 500- and 833-ms thresholds) increases with interval length. (b) Depiction of Eq. (5), which describes the relationship between intersaccade interval (I), interstimulus interval (ISI), and latency (L). (c) The difference in duration between consecutive intersaccade intervals plotted as a

function of latency for a sample subject. The latency in this example is the error experienced between the two intervals. Mean latency (-72 ms) is represented by the vertical black dashed line; the red dashed line is the linear regression fit to the data (slope -2.2). There is a significant negative linear relationship between the two measures ($R^2 = -0.8, P < 0.001$) suggesting that only the most recent error affects the next intersaccade interval duration

The operation of the model is outlined in the caption to Fig. 7 and briefly here, before the more detailed description below. In the model, the timing between eye movements is based on an internal estimate of stimulus timing (an internal clock), which is implemented as a (noisy) signal integrated to a variable threshold. The interval estimate, which determines the timing between saccades, is set by the threshold of the integrate-to-fire mechanism; this threshold is adjusted by feedback of the timing (intermovement intervals) and error (latency) of previous movements made within a correlation window of approximately 2 s.

Previous studies have modeled time estimation in the form of a linearly increasing signal, which triggers an event when a threshold level is reached (Schöner 2002). This is the central timing mechanism of our model as well. In this paper, we formulate this process as a signal $u(t)$ that increases linearly with additive noise:

$$u(t) = ft + u(0) + W(t) \quad (1)$$

$$W(t) = W(t-1) + n(t); W(0) = 0 \quad (2)$$

$$n(t) \sim N(0, \sigma_w). \quad (3)$$

In these equations, ft represents the linear rise of the signal (with slope f , 1 ms^{-1}). Additive noise is in the form of a Wiener process, $W(t)$, which is a continuous-time Gaussian stochastic process with independent increments: $N(0, \sigma_w)$ is Gaussian with a mean of 0 ms and standard deviation, σ_w , of 5 ms. We chose a noise level (standard deviation) of 5 ms, since this represents an approximate

lower limit to the interval at which two consecutive visual stimuli can be distinguished (Artieda et al. 1992). Thus, 5 ms is within the noise level of the neural timing system when timing information is provided by a visual stimulus. Figure 6(a) displays an example of five integrated signals rising to threshold for the time estimation of 500, 833, and 1,000 ms (physical time). Due to random fluctuations in the signals, the time when an event occurs (the signal crossing the threshold) is a random variable. The higher the threshold level, the larger is the variance of the times when the signal crosses threshold. In terms of timing behavior, this provides larger variance in the estimation of longer intervals (as demonstrated in Fig. 4(a)).

The complete timing model, which is depicted in Fig. 7, was constructed in the following manner (numbers in parentheses correspond to the graphics in the figure). Based on previous results on repetitive saccades (Stark et al. 1962; Ross and Ross 1987; Zambardi et al. 1987; Shelhamer and Joiner 2003; Isotalo et al. 2005; Joiner and Shelhamer 2006a, b) and tapping (Mätes et al. 1994; Engström et al. 1996; Miyake et al. 2004), when the pacing of the stimulus is slow, the ISI is large, there is no estimation of the target timing (1), and a reactive response is made after the stimulus jump (the delay of the eye movement, Δ) (2) (this is also the case for the first two movements to the alternating stimulus even at a smaller ISI; the subject can only estimate the timing of the stimulus and the required timing between movements, after experiencing at least one complete intersaccade interval [two movements]).

As previously described, subjects make predictive responses (4) to targets alternating at small ISIs (3). In addition to demonstrating the scalar property at these pacing rates (Fig. 4(b)), recent studies of predictive

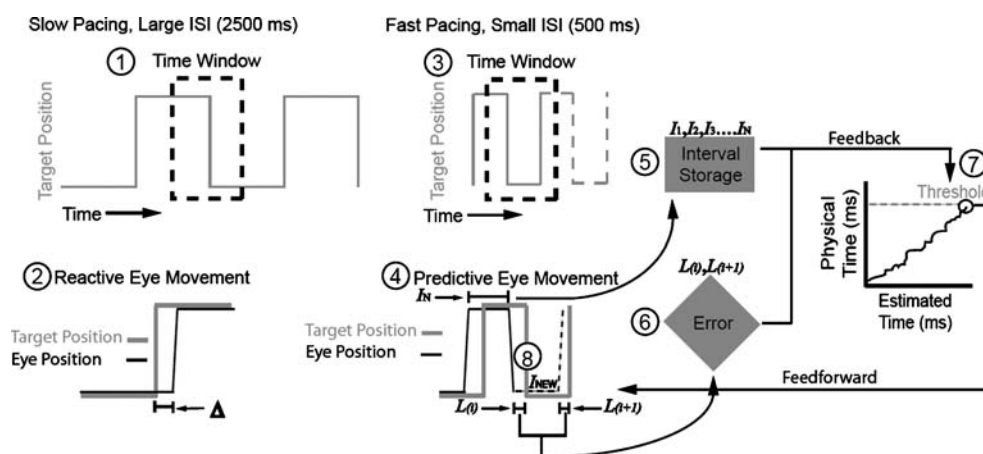


Fig. 7 Block diagram of the model. When the ISI is large (I), consecutive stimulus jumps do not fall within the time (correlation) window (black dashed-lined box). Thus, there is no estimation of the stimulus timing; a reactive response (delay Δ) is made (2). When the ISI is small, consecutive target jumps fall within the time window (3) resulting in predictive responses (4). Time estimation is modeled as a

linearly rising signal to threshold with added noise. The timing of future movements, I_{NEW} (8), is based on previous intervals ($I_1, I_2, I_3, \dots, I_N$) (5). The threshold (7) used to estimate I_{NEW} is increased or reduced by the most recently experienced error or latency, $L(i)$, and the projected future error, $L(i+1)$ (6)

saccades have shown that there are strong correlations between trials within a window of approximately 2 s (Shelhamer 2005). This suggests that when two or more previous movements fall within a time window (correlation window) of about 2 s, there can be an estimate of target timing (ISIs) (3) and feedback from the movements made within this window to adjust the timing of future movements. Our goal was to develop a model that produces the correct timing between movements (intersaccade interval) and also minimizes the error between the stimulus and the eye movement response resulting in a predictive latency. The intersaccade interval (I) can be represented in terms of the ISI and latency (L):

$$I(i) = \text{ISI}(i) - L(i) + L(i + 1). \tag{4}$$

This scheme is depicted in Fig. 6(b). When the two latency terms are equal, the timing of the stimulus and the response are equivalent. When the timing of the response and the stimulus are not the same ($I(i) \neq \text{ISI}(i)$), this is because the latency at the start of a given interval, $L(i)$, and the latency at the end of the interval, $L(i+1)$, are not the same. The model corrects for such errors in timing by estimating the appropriate values of latency and interval and using these errors to adjust the duration of the subsequent intersaccade interval. This adjustment is done by changing the threshold of the integrate-to-threshold mechanism. This is a key feature of the model: latency errors are monitored and used to adjust intersaccade intervals. Latency is a physiologically relevant error which should be reduced, while intervals are the controlled quantity in a predictor/clock model.

More specifically, in the model, I is a manifestation of the threshold for the time estimation process (for example, the green line in Fig. 6(a)), which is determined by $\text{ISI}(i)$, $L(i)$, and $L(i+1)$. With the appropriate scaling of these variables for mathematical convenience, we can make the threshold directly dependent on these quantities:

$$\text{threshold} = \text{ISI}(i) - L(i) + L(i + 1). \tag{5}$$

We now describe how the three quantities on the right side of this equation are estimated in the model. Although we describe how our mathematical model accomplishes these tasks, we note that these computations are neurally plausible. While we do not suggest specific neural mechanisms, neither do we propose any processes that would be unreasonable for a neural system to perform. First is the estimate of the ISI, $\text{ISI}(i)$, whose exact duration is unknown to the subject. This duration, however, can be approximated by neural processing in the subject as the average of previous intersaccade intervals, specifically those that occur

within the correlation window of previous movements ($I_1, I_2, I_3, \dots, I_N$) (5):

$$\text{ISI} \approx \frac{\sum_{i=1}^N I_i}{N}. \tag{6}$$

In this equation, I_N is the most recent interval, and I_1 is the least recent interval within the window. This storage and averaging (with constant weighting) of previous intervals is plausible given the fact that it is a motor act that is being accumulated: we consider it likely that the nervous system can hold and integrate intervals that is has *produced* (rather than merely *sensed*) with high fidelity. Since these intervals are the result of motor acts generated by the brain, it would appear to be a simple matter to maintain an efference copy of these intervals for further processing.

Next, this estimate of the required interval must be adjusted by previous errors. For example, if the intersaccade intervals were fixed at 450 ms with an ISI (target interval) of 500 ms, the location of the eye movements would be completely out of phase with the stimulus location by the tenth movement. Based on Eq. (4), the interval estimate is adjusted by the most recently experienced error or latency, $L(i)$, and the projected future error, $L(i+1)$ (6). Though multiple past errors could conceivably influence the interval estimate, we have experimental evidence that suggests that only the *most recent* previous error (latency) affects the next intersaccade interval. The relevant results for a sample subject are presented in Fig. 6(c). When the difference in duration between consecutive intersaccade intervals is plotted as a function of latency, there is a significant negative linear relationship ($R^2 = -0.8$, $P < 0.001$; this latency is the error experienced between the two intervals; in terms of Eq. (5), Fig. 6(c) plots $I(i) - I(i-1)$ vs $L(i)$). In other words, when the error is less than the mean latency (represented by the dashed vertical black line in Fig. 6(c), -72 ms), the subject increases the duration of the next interval. When the error is more than the mean latency, the subject decreases the duration of the next interval. This change in duration is near 0 ms at the mean latency, where no change is needed. It is interesting to note that the significance and magnitude of this relationship quickly decrease when the change in duration is compared to errors occurring earlier within the sequence (data not shown), confirming our contention that these errors have little or no influence over the adjustment of subsequent intervals.

Unlike $\text{ISI}(i)$, the most recently experienced error, $L(i)$, can be detected visually by the subject with no need for long-term storage and is represented in the model as the latency with added noise, $N(0, \sigma_N)$ (as with the time

estimation process, the noise is Gaussian with a mean of 0 ms and standard deviation, σ_N , of 5 ms):

$$L(i) \approx L(i) + N(0, \sigma_N). \quad (7)$$

The projected future latency must be estimated through a less direct process, since it is manifest at the end of interval $I(i)$, which has not yet occurred when the estimate is needed: $L(i+1)$ is thus the anticipated error resulting from the duration of the estimated intersaccade interval. This error is posited to be represented in the brain as a Gaussian distribution based on predictive tracking experience. For the model, its parameters were determined from experimental data obtained during steady-state predictive tracking, $N(\mu_{\text{prediction}}, \sigma_{\text{prediction}})$ (the determination of the mean, $\mu_{\text{prediction}}$, and standard deviation, $\sigma_{\text{prediction}}$, of this distribution is described in the following section).

Altogether, the threshold can now be represented as a combination of the estimates just discussed:

$$\text{threshold} = \frac{\sum_{i=1}^N I_i}{N} - L(i) + N(0, \sigma_N) + N(\mu_{\text{prediction}}, \sigma_{\text{prediction}}). \quad (8)$$

The time that $u(t)$, representing time estimation, reaches this threshold (7), sets the timing of the future movement, I_{NEW} (8). Once this threshold is reached, $u(t)$ is reset to zero, and the time estimation process begins again. Thus, our model utilizes a *response reset* strategy in which the next intersaccade interval during predictive tracking is timed from the previous movement response (Hary and Moore 1987a; Schulze 1992).

The simulation of this model was done on a PC using MATLAB™.

2.4 Determination of model parameters from behavioral data

Previous studies of normal human subjects tracking alternating targets (Stark et al. 1962; Ross and Ross 1987; Zambardi et al. 1987; Shelhamer and Joiner 2003; Isotalo et al. 2005; Joiner and Shelhamer 2006a, b) have demonstrated that there are distinct pacing rates, ISIs, that promote high-latency-reactive tracking (ISIs ranging from 1,250 to 2,500 ms) or low-latency-predictive tracking (ISIs ranging from 500 to 625 ms). Our earlier experiments (Shelhamer and Joiner 2003; Joiner and Shelhamer 2006b) reported a behavioral “phase transition” as subjects tracked alternating targets as ISI monotonically decreased. When subjects tracked the targets alternating at a large ISI (2,500 and 1,667 ms), they made reactive eye movements (latency ~180 ms). As the ISI monotonically decreased, subjects made an abrupt transition at a critical

ISI (near the ISI of 714 ms) to a predictive response (latency < 80 ms) and continued this behavior at the small ISIs (556 and 500 ms). This behavioral transition in tracking behavior is depicted for three subjects in panels (a), (b), and (c) of Fig. 3. The circles in each panel represent the saccade latency for a single trial/target jump. The thick black X is the average saccade latency for a given ISI. The solid and dashed black lines represent an abrupt transition fit and linear regression fit to the data. The transition fit (fitting two lines with zero slopes to the reactive and predictive ranges) is a significantly better representation of the data than is the linear fit (see Shelhamer and Joiner 2003; Joiner and Shelhamer 2006b). As demonstrated in each panel, saccade latency makes a rapid transition from reactive (approximately 200 ms) to predictive (< 0 ms) as the ISI decreases. The point of transition is different for each subject; panel (a) 833 ms, panel (b) 1,000 ms, and panel (c) 1,667 ms.

The results of this experiment can be utilized to determine parameter values in the model simulation. For example, the critical ISI for the behavioral transition from reactive to predictive tracking marks the point at which target jumps (and saccades) occur sufficiently rapidly for the subject to begin predicting: predictive tracking can begin when at least two previous intersaccade intervals fall within the correlation window (so that a reasonable estimate of ISI can be made, from these two intersaccade intervals). As explained below, this transition point can be used to provide an estimate of the correlation window size over which subjects utilize the feedback of previous movements.

The autocorrelation function of the predictive latency time series provides another way to estimate the size of the correlation window over which past performance is monitored. As in previous work (Shelhamer 2005; Joiner and Shelhamer 2006c), we set a threshold value for “significant” correlation and define a “correlation window” over which the latencies of past saccades are “significantly” correlated. In particular, we set the threshold for significant correlation at $R_{LL}=0.2$, and determine when the latency autocorrelation function R_{LL} crosses this threshold; this is indicated as the set of horizontal bars in panel (d) of Fig. 3, which shows the autocorrelation functions for the same three subjects presented in panels (a), (b), and (c) (red, green, and blue, respectively). The autocorrelation functions for each subject were determined from the latency time series at 0.9 Hz pacing for 300 trials. The differences in the autocorrelation functions reflect different correlation windows across subjects.

In panel (e) of Fig. 3, we compare these two ways of estimating the size of the correlation window. The mean and standard deviation of the intersaccade intervals made at the critical ISI, obtained from the phase-transition experiment, are plotted against the correlation window span,

obtained from the autocorrelation function of the predictive latency time series for seven subjects. The data are grouped around the equality line, demonstrating a correspondence between the two estimates of the correlation window size. Thus, we have two related estimates of the window length, which were derived independently based on observations on different sets of data. We should note that the mean and standard deviation of the intersaccade interval data at the point of the behavioral phase transition are here scaled by a factor of two; this implements the fact that, as stated in Section 1, the timing of the stimulus can only be estimated after two movements (Fig. 1(b)), and it is only on the next (third) and subsequent movements that this information can be utilized in programming saccade initiation time (see Joiner and Shelhamer 2006a). In other words, though predictive tracking can begin when two movements fall within the correlation window, the timing between these two movements is not an estimate of the correlation window size. The correct estimate is this timing scaled by a factor of two because it is only on the next movement that this estimation can be utilized. This is further supported by the relationship between latency and the difference between consecutive intersaccade intervals presented in Fig. 6(c). It is this realization that led us to investigate the relationship described in Fig. 3(e), which suggests that subjects make the transition from reactive to predictive tracking when two consecutive movements fall within the correlation window and that the correlation window size is approximately twice the duration of the movement timing demonstrated at the transition.

Two final experimental observations have a bearing on parameters in the model. First, as described previously and in more detail in Section 3, the correlation window increases with tracking experience (Fig. 5(b)). We model this as a linear increase in the size of the window as a function of the number of predictive saccades.

$$\text{window} = N(\mu_{\text{window}}, \sigma_{\text{window}}) + \beta N_p. \quad (9)$$

In this equation, μ_{base} and σ_{base} are the initial size and variability of the correlation window (the mean and standard deviation of the time window are estimated by the scaled intersaccade interval distribution at the reactive–predictive transition in tracking behavior during the phase-transition experiment), β is the growth rate of the window size (determined from the extended tracking experiment described in Section 3), and N_p is the number of previously experienced predictive saccades.

The second experimental observation involves the steady-state reactive and predictive tracking behavior observed during the phase-transition experiment. The latency data in the reactive range of the phase-transition experiment (immediately before the first and after the second behavioral transition) are used to estimate the

distribution of the latency (or delay, Δ) of reactive saccades that occur when the timing of the stimulus is outside the correlation window. As mentioned previously, the latency data when predictive saccades are made (immediately after the first and before the second behavioral transition) are used to determine the parameters ($\mu_{\text{prediction}}$ and $\sigma_{\text{prediction}}$) of the Gaussian distribution of the projected future error, $L(i+1)$.

3 Results

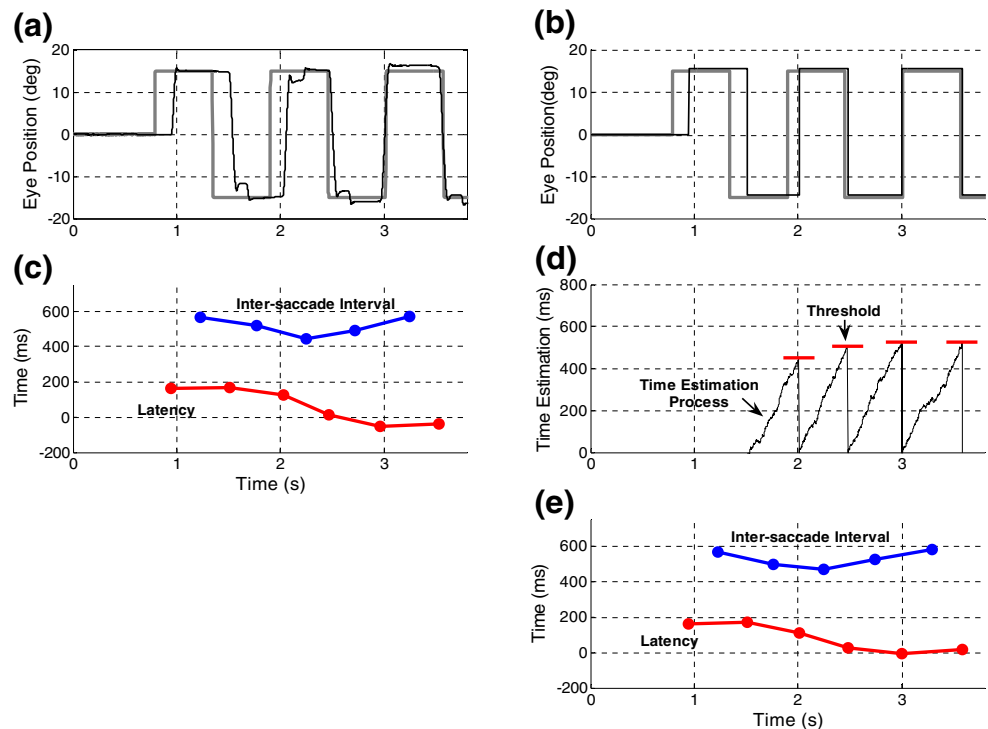
3.1 Experiment: extended tracking

Autocorrelation functions for predictive tracking latencies (approximately 1,000 trials at 0.9 Hz pacing) for one subject are presented in Fig. 5(a). The latency data were divided into four segments of approximately 250 trials each, and the four autocorrelation functions (colored traces) are based on these four segments; the black trace is the autocorrelation function for the entire data set. As demonstrated in the figure, correlation window lengths (estimated by the width of the autocorrelation functions at a level of 0.2 as represented the horizontal lines, see Section 2) increased as the respective segment occurred later in the data set. The correlation window lengths for the five autocorrelation functions presented in Fig. 5(a) are plotted as a function of consecutive trial number in Fig. 5(b). A logistic function fit (gray dashed line) represents the increase in time window length across all segments ($R^2=0.96$, $P=0.02$). However, over a smaller range (500 trials), a linear fit over the first three segments (black dashed line) is a sufficient representation ($R^2=0.96$, $P=0.19$). Utilizing this linear relationship, we determined the growth rate of the window size, β , as a function of number of predictive trials, N_p . For example, setting β to 0.0025 s per trial, 40 predictive trials equates to an increase of 100 ms in the correlation window length. We make use of this simplified linear fit in the development of our model, since it encompasses the data set sizes on which other aspects of the model are based.

3.2 Model

A comparison of normal subject and simulated predictive saccade-tracking behavior is presented in Fig. 8. The same data presented in Fig. 1(a) for a sample subject are displayed again in panel (a) of Fig. 8. Panel (b) plots the change in latency and intersaccade interval throughout the data displayed in panel (a). As described in Section 1, when the subject begins to track the alternating targets, the first two saccades are reactive (they occur after the stimulus jump with respective latencies of 161 and 166 ms). By the

Fig. 8 (a) The predictive tracking behavior (eye and target position, *black* and *gray* traces, respectively) for the sample subject presented in Fig. 1(a). (c) The change in latency (*red* trace) and intersaccade interval (*blue* trace) for the data presented in (a). (b) The simulated results for the same stimulus pacing rate (an ISI of 556 ms) utilized in (a). (d) The noisy internal counter signal (*black* trace, see Fig. 6(a)) integrated to threshold (*horizontal red bars*) for the simulation presented in (b). (e) The change in latency and intersaccade interval throughout the simulated data presented in (b) and (d)



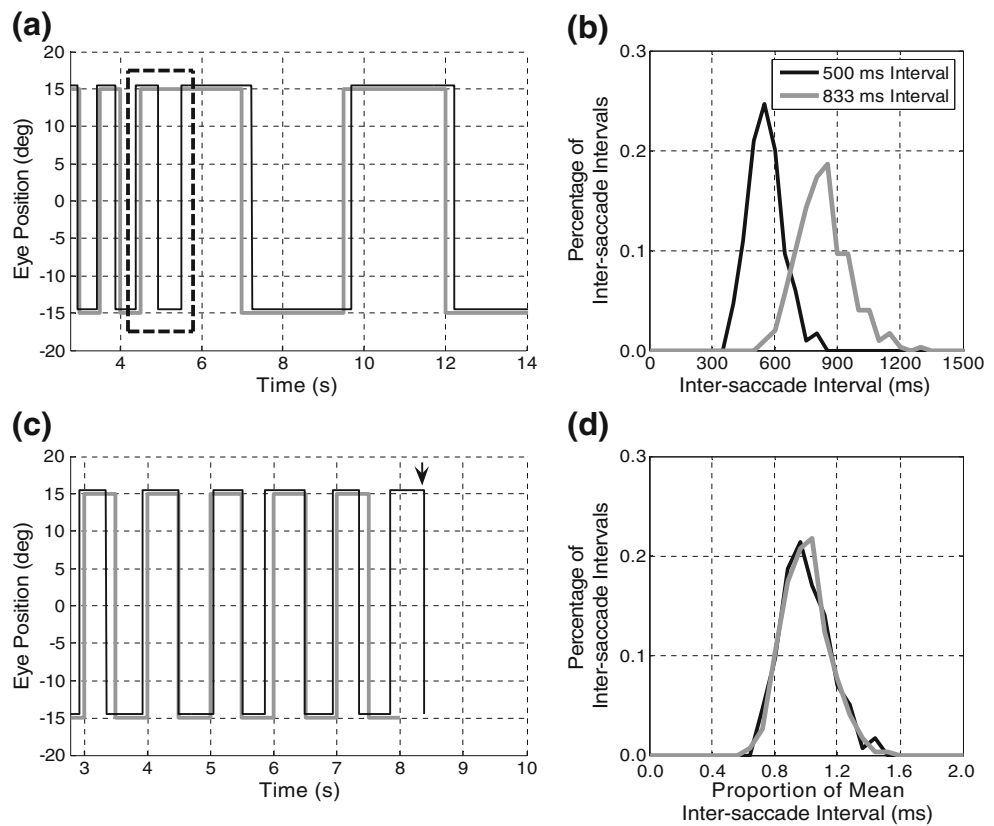
fourth movement, the subject's eye movement occurs with a latency of 12 ms signifying that it is a preplanned predictive movement. To overcome the initial timing error (the first two reactive movements), the subject must decrease the intersaccade interval. These changes are displayed in panel (c): latency begins near 200 ms and decreases to approximately 0 ms by 2.5 s. Correspondingly, the intersaccade intervals begin near 550 ms, decrease to approximately 400 ms at 2.2 s, and rise again to 550 ms.

The simulation results for the same stimulus pacing rate (an ISI of 556 ms) are displayed in panels (b), (d), and (e) of Fig. 8. In panel (b), the simulated results are displayed in the same format as the eye and target position traces presented in panel (a). The repetitive noisy internal-counter signals and respective thresholds for the simulated data in panel (b) are displayed in panel (d) (the noisy signals in panel (d) are the same as those described in Fig. 6(a)). There are three important aspects of the model that are displayed in panel (d) that should be noted. First, the internal estimation begins only after the first two saccades; at least one intermovement interval is required for time estimation. Second, the threshold for the internal estimation changes based on feedback (see Section 2); the vertical positions of the red bars change throughout the simulation. Third, the *response reset* strategy (the next intersaccade interval is timed from the last movement response) described in previous reports (Hary and Moore 1987a; Schulze 1992) is demonstrated; the noisy signal is reset to zero after the threshold is reached. The changes in latency

and intersaccade interval throughout the simulation are presented in panel (e). It is important to note that these aspects of the simulation resemble those of the sample subject (panel (c)): to overcome the initial initiation-timing error (the first two reactive movements), the intersaccade interval is decreased and then increased once the latency has been reduced.

The predictive-timing model was presented with the same stimulus timing (ISIs) as were the subjects in the experiments presented in Figs. 2 and 3. The model performed similarly to these normal subjects when the timing of the stimulus was abruptly changed. For example, to simulate the perturbation experiment (Fig. 2(a)), the model was presented with ISIs that suddenly changed from small to large (500 to 2500 ms). In the simulation (Fig. 9(a)), the model continued to produce movement timing at the preperturbation rate despite the increase in ISI. This is due to the model estimating the timing of future movements based on previous trials. When the error of previous trials exceeds the tolerable error (more than the estimated ISI), the model reverts to a reactive mode as shown by the simulated eye movement occurring after the stimulus jump (for example, the eye movement that occurs at approximately 7 s). Similar to the observed behavior when subjects track alternating targets that are abruptly extinguished (Fig. 2(b)), when the model is presented with several cycles of a small ISI (500 ms) that abruptly end (Fig. 9(c)), the preprogrammed movements continue in the absence of a visual stimulus.

Fig. 9 When presented with stimulus timing (*gray trace*) that abruptly changes (small→large ISI, **(a)**) or stops (**(c)**), the model continues to produce movement timing (*black trace*) at the pre-existing predictive pacing rate. In **(a)**, this continuation of predictive tracking despite the stimulus perturbation is *highlighted* within the *dashed box*. In **(b)**, the continuation is marked by the *downward arrow*. **(b)** When presented with a constant ISI of 833 or 500 ms, the time between the simulated movements varies around the ISI, and the standard deviation increases with ISI. **(d)** Simulated distributions demonstrate the scalar property when divided by the mean interval



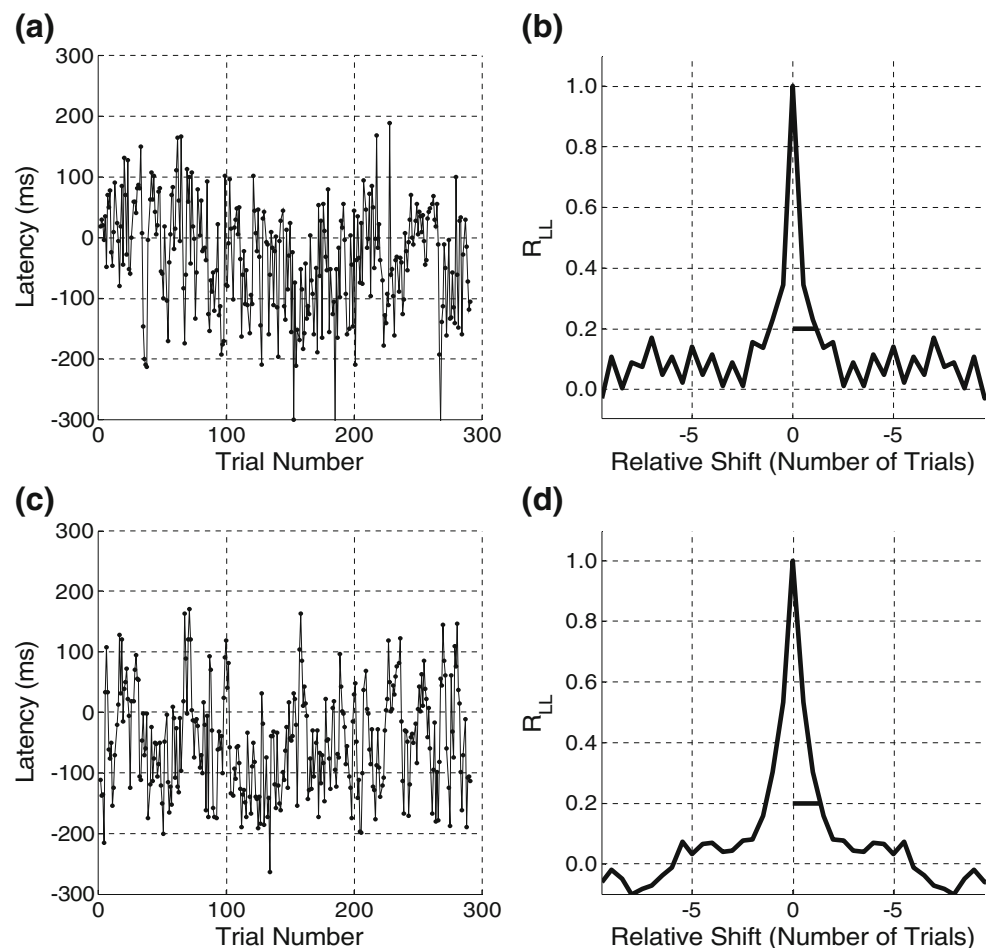
Evidence that subjects utilize the same internal-timing mechanism during predictive tracking at different pacing rates was provided by the scalar property: timing variance (intersaccade interval standard deviation) increased proportionally with interval length (Fig. 4(a)). As a result, normalized intersaccade interval histograms for different ISIs overlap (Fig. 4(b)). To determine if the simulation also demonstrated this property, the model was presented with ISIs of 500 and 833 ms for 300 trials each. The simulated intersaccade intervals produced by the model are distributed around the ISI, and the variability (width of the distribution) increased with interval length (Fig. 9(b)). These distributions also demonstrate the scalar property when they are divided by the mean interval (Fig. 9(d)).

We also wished to compare the simulated steady-state predictive tracking to normal subject behavior. Specifically, we wished to demonstrate that the statistics (mean, variability, and correlation structure) of the simulated tracking resembled that of normal subjects. The latency time series for tracking at an ISI of 556 ms for 300 trials is plotted in Fig. 10(a) and (c) for a sample subject and for the simulation. The mean and standard deviation of the latency (-29 ± 93 and -49 ± 89 ms) and the intersaccade intervals (556 ± 102 and 556 ± 84 ms) were comparable between the experimental and simulated time series. Additionally, the

shape of the autocorrelation functions of the latency time series (panels (b) and (d) for the subject and simulation, respectively) were similar and yielded comparable estimates of the correlation window size (1,300 and 1,500 ms, respectively).

In addition to simulating the behavioral results listed above, the model demonstrates the behavioral phase transition in tracking behavior. As described in Section 2, there is an abrupt “phase transition” from reactive to predictive tracking behavior when the ISI begins large (2,500 ms) and monotonically decreases to a small value (500 ms). In addition, there is hysteresis in this behavior as the ISI subsequently increases monotonically: subjects continue to predict the target jump at ISIs that initially promoted reactive movements. This hysteresis is demonstrated in Fig. 11(a) and (c) for one subject (the same subject presented in Fig. 3(a)). The direction of the ISI change (monotonically increasing or decreasing) is indicated by the direction of the arrow. The individual latency values are plotted as a function of ISI along with their mean. Mean latency varies in a systematic manner with ISI. During the ISI decrease (panel (a)), mean latency at the largest ISIs (2,500–1,000 ms) is almost constant at 150 ms, indicating that the subject is reacting to each target jump with a “normal” saccade latency. At the ISI of 833 ms, the subject undergoes a transition between tracking states and

Fig. 10 Latency time series for tracking at an ISI of 556 ms for 300 trials for (a) a sample subject and (c) simulation. Autocorrelation functions for the respective latency time series are shown in (b) and (d)



makes predictive movements after this point: At the smallest ISIs (714–500 ms), mean latency is near constant at -85 ms, signifying that the subject is making saccades in a predictive manner, in anticipation of each target jump. Latency data for the same subject, as ISI subsequently increased, are shown in Fig. 11(c). The subject predicts the target jump at the four smallest ISIs (833–500 ms), with a mean latency of -105 ms. At the ISI of 1,000 ms, there is a transition from predictive to reactive tracking. It is important to note that ISI at this transition point is greater than that at the previous transition (833 ms)—that from reactive to predictive as ISI decreased (Fig. 11(a); the method by which these transition points were statistically verified is described in Joiner and Shelhamer 2006b). After this transition, tracking behavior is steadily reactive at the two largest ISIs (2,500 and 1,667 ms), with a mean latency of 120 ms. When presented with the same monotonic change in stimulus timing (large \rightarrow small \rightarrow large ISI), the model simulated the same hysteresis in tracking behavior: Behavioral phase transitions are made at ISIs of 833 and 1,000 ms for ISI decreasing and increasing (panels (b) and (d), respectively). This hysteresis is a natural consequence of the

increase in size of the correlation window with repeated predictive tracking (Fig. 5(b)): The window increases in duration after many cycles of predictive saccades, and the larger window can contain two movements at a larger ISI than is initially the case.

One final result relates to the statistical structure of the intertrial correlations (which are manifest by the gradual decay of the autocorrelations of consecutive saccade latencies, as in Figs. 5 and 10). Our previous work (Shelhamer 2005) showed that the correlations decay as a power law: The autocorrelation of the latency series has the form of $R_{LL} \sim \tau^{-b}$ where τ is the relative shift (in trials), and the power spectrum of the same data has the form of $S_{LL} \sim f^{-\alpha}$ (this is not the case for reactive saccades). Figure 12 shows the autocorrelation functions and power spectra for two implementations of the current model: As described above (panels (c) and (d)) and without the modulation of the correlation window as described by Eq. (9) (i.e., $\beta=0$; panels (a) and (b)). In both cases, the results suggest a correlation structure as found in our previous work in behavioral data (e.g., Fig. 5): power law decay of autocorrelation, $1/f$ type of spectrum. However, the

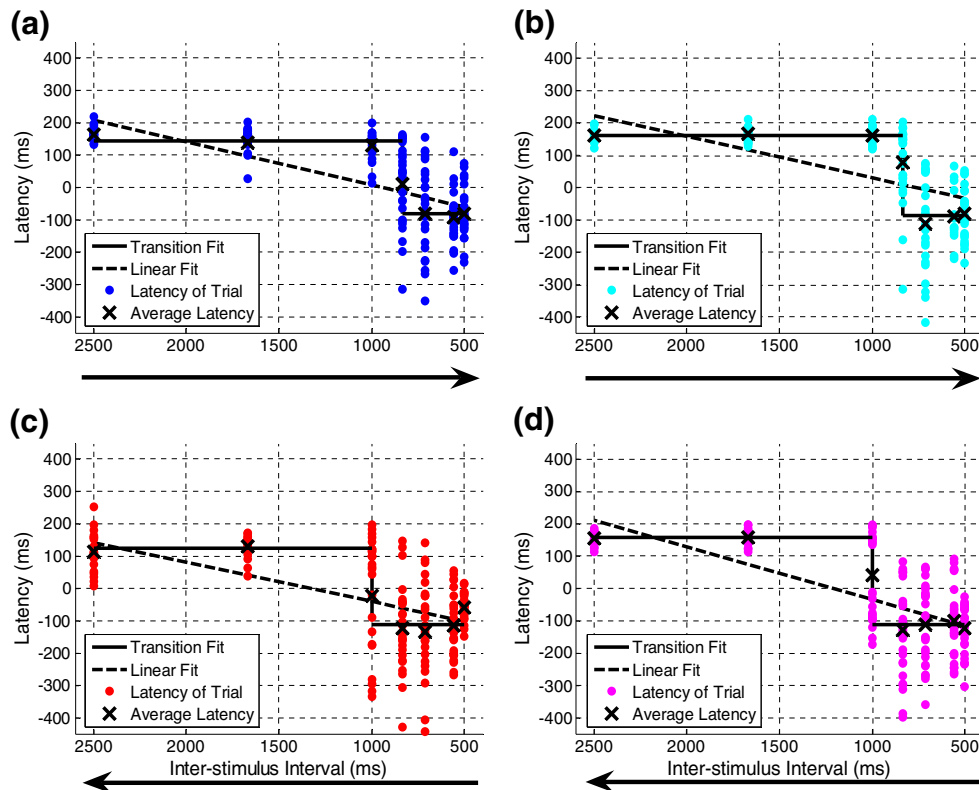


Fig. 11 Experimental and simulated results during the phase-transition paradigm. The direction of the ISI change (monotonically increasing or decreasing) is indicated by the *arrow*. At each discrete ISI, the latency of each primary saccade is plotted as a single point; *X* represents the mean latency at a given ISI. (a) Saccade latency as a function of decreasing ISI for one subject (the same subject presented in Fig. 3(a)). A *straight line* was fit to the latency data via linear regression (*dashed line*), which represents the hypothesis of a smooth change in latency with interstimulus interval. A “transition fit” was also made, in which data in the reactive range (2,500–1,000 ms) and

in the predictive range (714–500 ms) were fit with separate *horizontal lines* through the two group means; this represents the hypothesis of an abrupt “phase transition” in latency as a function of ISI, at the ISI of 833 ms. (c) Layout and interpretation as for (a) for increasing ISI. Transition fit in this case is based on a transition at 1,000 ms. When presented with the same monotonic change in stimulus timing (large→small→large ISI), the model simulated the same hysteresis in tracking behavior: Behavioral phase transitions are made at ISIs of 833 and 1,000 ms for (b) ISI decreasing and (d) increasing, respectively

implementation of the dynamic window modulation based on experience (panels (c) and (d)) produces what appears to be a better spectral fit; note especially deviations from the best-fit straight line (gray line which represents $1/f^\alpha$ on a log–log plot) at lower frequencies with the static window ((a) and (b)). Possible reasons for this discrepancy are discussed below.

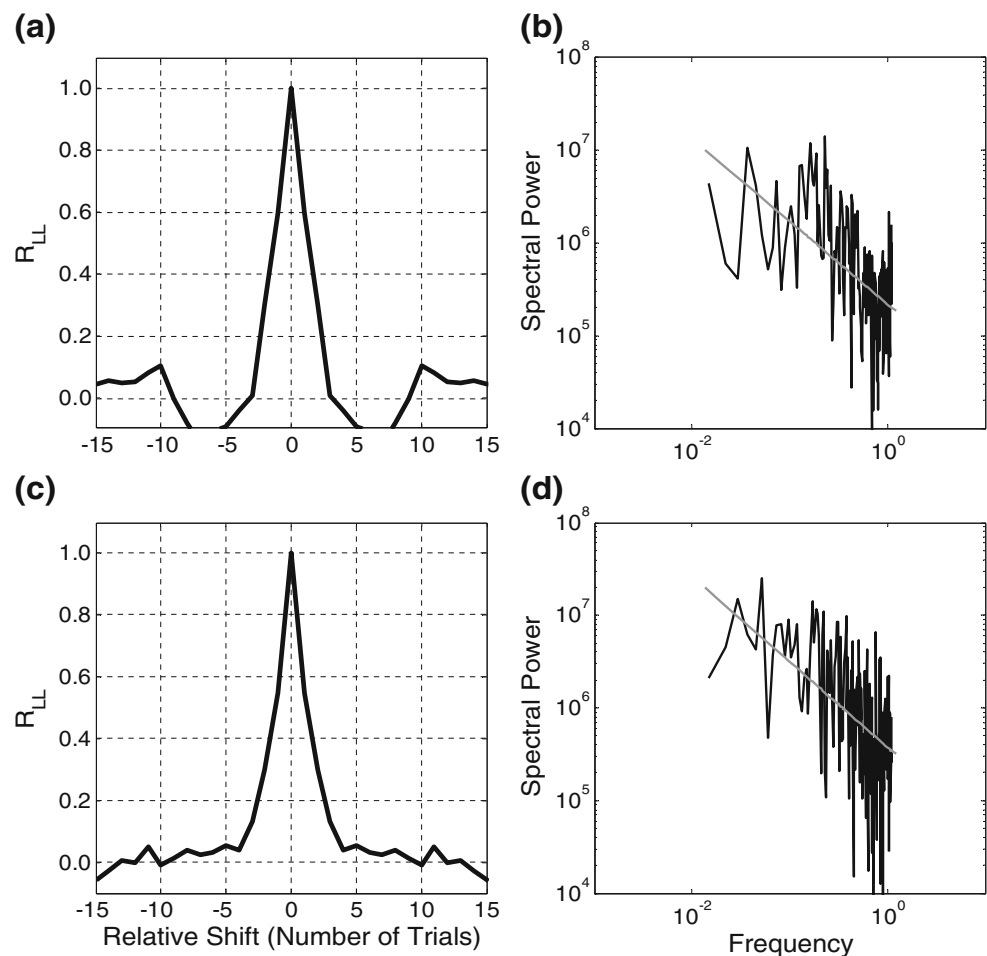
4 Discussion

4.1 Comparison to previous models

As stated in Section 1, there are several previous models of motor synchronization to a pacing stimulus. We believe that the model presented in the current manuscript is novel for several reasons. First, whereas other models restricted feedback to a predefined number of previous movements (Michon 1967; Hary and Moore

1985, 1987a, b; Vos and Hlsper, 1992; Mates 1994a, b), the feedback used in our model is gathered over a temporal window (correlation window) of previous performance. Next, the model combines aspects of the internal clock framework (Treisman 1963; Gibbon 1977; Meck and Benson 2002) with the monitoring of previous movements within a temporal window. In our model, predictive saccade tracking is based on an internal clock (internal estimation of the stimulus timing represented by the integrate-to-fire mechanism), the duration (threshold) of which is modified by feedback from previous intersaccade intervals and recent and projected timing errors (latencies). Third, the model reproduced a number of different behavioral results (change from reaction to prediction on initial tracking, phase transition, hysteresis, scalar property, continuation of predictive tracking despite perturbations, and intertrial correlations) with very few basic principles, while other timing studies and models have addressed these issues more or less independently

Fig. 12 Simulated results on intertrial correlations. **(a)** Auto-correlation function for model data, with a static correlation window ($\beta=0$ in equation 9). **(b)** The power spectrum of the data used in **(a)**. **(c)** Autocorrelation function from model data with a correlation window that varies with experience ($\beta=0.0025$ in equation 9). **(d)** The power spectrum of data in **(c)**. Both autocorrelations show a gradual decay, consistent with the power law behavior. However, the power spectrum in the case of the varying window is better approximated by a $1/f^\alpha$ form (gray straight line)



(see Schöner 2002; Matell and Meck 2004; Mauk and Buonomano 2004; Buhusi and Meck 2005). For example, previous models have taken a more theoretical approach in quantitatively describing behavioral phase transitions (Haken et al. 1985; Schöner et al. 1986; Jirsa et al. 1994; in these studies, the models describe the transition between two coordinative patterns of the hands rather than timing and describe the transition in terms of oscillators). In the present model, the behavioral phase transition in timing behavior is due to the width of the correlation window; reactive or predictive tracking is dependent upon whether there is a sufficient amount of information (the number of movements) within the temporal window to estimate the stimulus timing. Though theoretical, this parameter of the model was determined experimentally. As described in Section 2, the duration of the window time span was estimated from two independent experiments, and the correspondence between the two estimates further suggests that the transition occurs when the timing information is sufficient. In addition, the behavioral hysteresis is a natural consequence of the widening of the window with extended predictive saccade tracking, another experimental finding.

4.2 Integrate-to-fire mechanism

There is recent evidence that temporal processing may not be centralized but rather distributed among different neural structures (Rao et al. 1997; Mauk and Buonomano 2004; Buhusi and Meck 2005). In our proposed model, the estimation of time is represented by a single integrate-to-threshold process. It is not our intent to suggest that the estimation of time is single centralized mechanism. Rather, we propose that the variability of time estimation, whether centralized or distributed, in the temporal range where subjects demonstrate predictive tracking behavior (approximately 500 to 1,500 ms) can be represented as a noisy integration process. The Gaussian distribution of the noise can be considered as the averaged effect of the many independent sources of variability that could arise from different neural areas (Gardiner 2004). Though we could have modeled time estimation as a process with a constant rise that varied from trial-to-trial, we chose the noisy integration process (the combination of a random walk process with a process that increased at a constant rate with time) for two reasons: (1) The neurobiological sources of variability throughout the time estimation process (Meck

and Benson 2002; Buhusi and Meck 2005) suggests that the rate is subject to noise, which is captured with the random walk process (Schöner 2002), and (2) the finding that the scalar property holds for repetitive predictive saccade sequences (Fig. 4) suggests that the longer this variability is integrated into the estimate, the more variability there is in the timing distribution (Fig. 6(a)).

This type of noisy integration process has successfully been utilized to describe some aspects of cognitive behavior. For example, Sigman and Dehaene (2005) utilized this mechanism to model the decision-making process and the resulting reaction time distributions from a dual task: Subjects performed a number classification task followed by a tone discrimination task. Though simple, the model made predictions that held over a range of task manipulations (i.e., presenting the numbers as digits or in spelled words), which enabled the authors to parse the task into serial and parallel components. In addition, similar theoretical models have been used to describe the reaction time of single reactive saccadic eye movements (LATER model: Carpenter and Williams 1995; Reddi and Carpenter 2000). Rather than the integration of a noisy signal, the process that initiates the eye movement in these studies is a linear accumulation to threshold with a growth rate that varies randomly from movement to movement. This rise-to-threshold behavior has been identified in single-neuron recordings of the frontal eye fields and superior colliculus (Hanes and Schall 1996; Hanes et al. 1998; Paré and Hanes 2003) and supports the theory of a trigger threshold in movement initiation.

4.3 Application to repetitive tapping movements

There are several behavioral similarities between repetitive tapping and saccades that suggest that the proposed model could also be applied to synchronized tapping. For example, repetitive tapping movements to a pacing metronome also demonstrate a behavioral phase transition from reactive to anticipatory as the ISI monotonically decreases (Engström et al. 1996). In addition, it has been previously proposed that synchronized tapping (anticipatory behavior) is based on a temporal integration of previous movements occurring within a time window of approximately 3 s (Mates et al. 1994). Thus, it is likely that the framework of the model described in the current manuscript (correlation window, feedback of timing error and intermovement interval, time estimation modeled as a noisy integration process) could also be applied to repetitive tapping movements. However, despite these behavioral similarities, there is an important difference between the two movements that may require adjustments to the model to adequately depict repetitive tapping. The timing error during repetitive tapping movements is sensed as tactile information as

opposed to the visual error during repetitive saccade tracking. This sensory difference may require a change in the feedback of the timing error. For example, an adjustment in the weighting of the previous and projected error may account for this difference between the two movements. In addition, differences have been found in the cortical representations of different effectors in the neural pathway for the transformation from sensory to motor signals (e.g., Calton et al. 2002; Lawrence and Snyder 2006), which suggests that different predictors/timers might exist for different effectors.

4.4 Intertrial correlations

Our latency data, both behavioral and simulated, show a statistical structure that resembles long-term correlations (often called “long-range dependence”). This is manifest as a gradual (power law) decay of the autocorrelation function and a $1/f^\alpha$ form of power spectrum. The implications of these long-range correlations have been discussed in many other contexts (for example Hausdorff et al. 1995; Linkenkaer-Hansen et al. 2001; Peng et al. 1995). While the most common explanation of these correlations is the interaction of many different neural processes acting on many different time scales, more recent work suggests that a more straightforward mechanism might be at work: Simple summation of a small number of random processes with different short-term time scales can produce time series that exhibit (or appear to) long-range correlations (Wagenmakers et al. 2004; Wing et al. 2004). One such formulation is white noise added to moving-average-filtered versions of white noise. This loosely resembles our implementation of the modulation of the correlation window with tracking experience (Eq. 9): intersaccade interval errors are monitored over the time specified by this window, and this window increases in size with extended predictive tracking.

It is important to note that though we use a distribution of predictive latencies as a parameter of the model, $L(i+1)$, the use of this data is not what produces the correlations between simulated trials (Fig. 10(d)). $L(i+1)$ is the projected error of the current interval estimate, I_{NEW} or threshold, and the values are drawn from this distribution (uncorrelated samples). Additionally, this latency value is only used in setting the threshold of the integrate-to-fire mechanism. In fact, it is the termination of the integrate-to-fire mechanism with respect to the stimulus jump that actually determines the error of the synchronization (for example, the latencies plotted in Fig. 10(c)). The intertrial correlations of the simulated data suggest that it is the influence of multiple previous intermovement intervals (not latency errors) within the correlation window that results in the correlations seen experimentally (Fig. 10(a)). One

question these results raise is how this source of timing information is encoded and stored. Recent findings suggest that the estimation of time passage may be accomplished by the accumulation of the action potentials emitted by dopaminergic neurons in the basal ganglia (Matell and Meck 2004). In addition, there is evidence that the storage of these time estimates may be mediated by the frontal and hippocampal systems (Meck et al. 1987).

Physiologically, we suggest that the increase in correlations with extended tracking, shown in Fig. 5, reflects the brain's increasing confidence in stimulus history: As pacing continues at the same rate, it is safe to use performance from further in the past in guiding future tracking. However, this might instead be an epiphenomenon of tracking performance becoming less variable with experience. While this is an interesting possibility, in fact, tracking performance does *not* typically become less variable with experience (data not shown). This raises the question of why the tracking system should bother to increase the correlation window if it does not lead to improved performance. We propose that building up a longer correlation window is an effective way to persevere storage of previous tracking, which is useful if predictive pacing is briefly interrupted or if experience must be pieced together from several short segments of consistent tracking. Another interesting question is how the size of the correlation window is determined and modulated with experience. We suspect that the window increases in size for each trial in which tracking error is below a tolerable limiting value. Evaluation of this idea is an aim of our future work.

While our results do not make a definitive statement as to the provenance or neurobiological role of these correlations, they do show that some aspects of our model—in particular the feedback of recent timing error and the real-time adjustment of the window over which this feedback takes place—can generate correlations that are similar to those that we find in behavioral data.

4.5 Relation to timing behaviors and neurological disease

While continuous tracking of periodic targets is not very biologically meaningful, we note that the model is based on these data but can reproduce the initiation phase of tracking—the first few saccades, a more biologically relevant situation. Furthermore, other types of rhythmic behaviors such as music and dance are biologically relevant for communication and socialization—any increase in our knowledge of timing behaviors in general could have a bearing on this understanding. For example, our model may contribute to the understanding of internally timed movements by its application to data acquired from patient populations that exhibit deficits in

the ability to produce anticipatory movements. Two likely neural structures involved in the internal estimation of time are the basal ganglia and the cerebellum (Harrington and Haaland 1999; Buonomano and Karmarkar 2002; Mauk and Buonomano 2004; Buhusi and Meck 2005). For example, patients with disorders of the basal ganglia exhibit deficits in predictive tracking of targets alternating at ISIs of approximately 1,000 ms (Bronstein and Kennard 1984, 1985; Crawford et al. 1989; Tian et al. 1991; Ventre et al. 1992). These deficits include an increase in timing variability and a decrease in the proportion of anticipatory responses compared to control subjects. In addition, patients with Parkinson's disease demonstrate an increase in timing variability during repetitive tapping that is attributed to an increase in internal clock variability rather than motor delay (Wing et al. 1984; Harrington et al. 1998). Based on the hypothesized involvement of the basal ganglia in the internal clock mechanism (see Matell and Meck 2004), this decrease in the percentage of predictive movements and increase in total timing variability may be replicated in simulation by increasing the noise added to the linear-rising signal.

The cerebellum has also been shown to play a critical role in rhythmic timing. Similar to Huntington's and Parkinson's disease patients, cerebellar patients display an increase in timing variability during rhythmic tapping to an auditory metronome pacing at an ISI of 550 ms (Ivry and Keele 1989; it should be noted that the ISI of 550 ms promotes anticipatory tapping behavior; Engström et al. 1996). These results are supported by the impairment of time perception in the millisecond range (400–600 ms) by induced disruption (via repetitive transcranial magnetic stimulation) of specific cerebellar regions (Koch et al. 2006; Lee et al. 2007). The cerebellum has also been shown to play a role in response timing adjustments. Dreher and Grafman (2002) demonstrated that the cerebellum is more active when subjects perform a task with timing irregularity rather than with constant timing. Similarly, a recent functional magnetic resonance imaging study (Schlerf et al. 2006) reported that specific regions of the cerebellum are involved in timing error correction. During a paced button press task, distinct regions of the cerebellum showed greater activity when the timing of the stimulus was variable rather than isochronous. These results suggest that the cerebellum may be involved in both the time estimation process and the feedback of inter-response intervals and timing errors. The increase in the intermovement variance by cerebellar patients during rhythmic finger tapping may be the result of damage to the timing error feedback mechanism. For example, adding random noise to the feedback of timing errors during the simulation (random fluctuations in the threshold of the internal counter) will also result in an increase

in the intermovement variance. Similar to the example described for Parkinson's patients, in this manner, it may be possible to attribute such functions as error feedback or time estimation during predictive repetitive movements to specific neural structures.

Acknowledgments The study was supported by NIH T32-MH20069 and EY015193 and NSF BCS-0615106.

References

- Artieda, J., Pastor, M. A., Lacruz, F., & Obeso, J. A. (1992). Temporal discrimination is abnormal in Parkinson's disease. *Brain*, *115*, 199–210.
- Bronstein, A. M., & Kennard, C. (1984). Predictive eye movements in normal subjects and in Parkinson's disease. In A. G. Gale & F. Johnson (Eds.), *Theoretical and applied aspects of eye movement research* (pp. 463–472). North Holland: Elsevier.
- Bronstein, A. M., & Kennard, C. (1985). Predictive ocular motor control in Parkinson's disease. *Brain*, *108*, 925–940.
- Buhusi, C. V., & Meck, W. H. (2005). What makes us tick? Functional and neural mechanisms of interval timing. *Nature Reviews Neuroscience*, *6*, 755–765.
- Buonomano, D. V., & Karmarkar, U. R. (2002). How do we tell time? *Neuroscientist*, *8*, 42–51.
- Burke, M., & Barnes, G. (2008). Brain and behavior: A task-dependent eye movement study. *Cerebral Cortex*, *18*, 126–135.
- Calton, J. L., Dickinson, A. R., & Snyder, L. H. (2002). Non-spatial, motor-specific activation in posterior parietal cortex. *Nature Neuroscience*, *5*, 580–588.
- Carpenter, R. H., & Williams, M. L. (1995). Neural computation of log likelihood in control of saccadic eye movements. *Nature*, *377*, 59–62.
- Chen, Y., Repp, B. H., & Patel, A. D. (2002). Spectral decomposition of variability in synchronization and continuation tapping: Comparisons between auditory and visual pacing and feedback conditions. *Human Movement Science*, *21*, 515–532.
- Collins, C. J., Jahanshahi, M., & Barnes, G. R. (1998). Timing variability of repetitive saccadic eye movements. *Experimental Brain Research*, *120*, 325–334.
- Crawford, T., Goodrich, S., Henderson, L., & Kennard, C. (1989). Predictive responses in Parkinson's disease: Manual keypresses and saccadic eye movements to regular stimulus events. *Journal of Neurology, Neurosurgery and Psychiatry*, *52*, 1033–1042.
- Dreher, J. C., & Grafman, J. (2002). The roles of the cerebellum and basal ganglia in timing and error prediction. *European Journal of Neuroscience*, *16*, 1609–1619.
- Engström, D. A., Kelso, J. A. S., & Holroyd, T. (1996). Reaction-anticipation transitions in human perception-action patterns. *Human Movement Science*, *15*, 809–832.
- Gagnon, D., O'Driscoll, G. A., Petrides, M., & Pike, G. B. (2002). The effect of spatial and temporal information on saccades and neural activity in oculomotor structures. *Brain*, *125*, 123–139.
- Gardiner, C. W. (2004). *Handbook of stochastic methods for physics, chemistry and the natural sciences*. Berlin: Springer.
- Getty, D. J. (1975). Discrimination of short temporal intervals: A comparison of two models. *Perception and Psychophysics*, *18*, 1–8.
- Gibbon, J. (1977). Scalar expectancy theory and Weber's law in animal timing. *Psychological Review*, *84*, 279–325.
- Gibbon, J., Malapani, C., Dale, C. L., & Gallistel, C. R. (1997). Toward a neurobiology of temporal cognition: Advances and challenges. *Current Opinion in Neurobiology*, *7*, 170–184.
- Haken, H., Kelso, J. A., & Bunz, H. (1985). A theoretical model of phase transitions in human hand movements. *Biological Cybernetics*, *51*, 347–356.
- Hanes, D. P., Patterson, W. F., & Schall, J. D. (1998). Role of frontal eye fields in countermanding saccades: Visual, movement, and fixation activity. *Journal of Neurophysiology*, *79*, 817–834.
- Hanes, D., & Schall, J. D. (1996). Neural control of voluntary movement initiation. *Science*, *274*, 427–430.
- Harrington, D. L., & Haaland, K. Y. (1999). Neural underpinnings of temporal processing: A review of focal lesion, pharmacological, and functional imaging research. *Reviews in the Neurosciences*, *10*, 91–116.
- Harrington, D. L., Haaland, K. Y., & Hermanowicz, N. (1998). Temporal processing in the basal ganglia. *Neuropsychology*, *12*, 3–12.
- Hary, D., & Moore, G. P. (1985). Temporal tracking and synchronization strategies. *Human Neurobiology*, *4*, 73–79.
- Hary, D., & Moore, G. P. (1987a). Synchronizing human movement with an external clock source. *Biological Cybernetics*, *56*, 305–311.
- Hary, D., & Moore, G. P. (1987b). On the performance and stability of human metronome-synchronization strategies. *British Journal of Mathematics and Statistical Psychology*, *40*, 109–124.
- Hausdorff, J. M., Peng, C. K., Ladin, Z., Wei, J. Y., & Goldberger, A. L. (1995). Is walking a random walk? Evidence for long-range correlations in stride interval of human gait. *Journal of Applied Physiology*, *78*, 349–358.
- Hoagland, H. (1933). The psychological control of judgements of duration: Evidence for a chemical clock. *Journal of General Psychology*, *9*, 267–287.
- Isotalo, E., Lasker, A. G., & Zee, D. S. (2005). Cognitive influences on predictive saccadic tracking. *Experimental Brain Research*, *165*, 461–469.
- Ivry, R. B., & Keele, S. W. (1989). Timing function of the cerebellum. *Journal of Cognitive Neuroscience*, *1*, 136–152.
- Jirsa, V. K., Friedrich, R., Haken, H., & Kelso, J. A. (1994). A theoretical model of phase transitions in the human brain. *Biological Cybernetics*, *71*, 27–35.
- Joiner, W. M., Lee, J. E., Lasker, A., & Shelhamer, M. (2007b). An internal clock for predictive saccades is established identically by auditory or visual information. *Vision Research*, *47*, 1645–1654.
- Joiner, W. M., Lee, J. E., & Shelhamer, M. (2007a). Behavioral analysis of predictive saccade tracking as studied by countermanding. *Experimental Brain Research*, *181*, 307–320.
- Joiner, W. J., & Shelhamer, M. (2006a). An internal clock generates repetitive predictive saccades. *Experimental Brain Research*, *175*, 305–320.
- Joiner, W. J., & Shelhamer, M. (2006b). Pursuit and saccadic tracking exhibit a similar dependence on movement preparation time. *Experimental Brain Research*, *173*, 572–586.
- Joiner, W. M., & Shelhamer, M. (2006c). Responses to noisy periodic stimuli reveal properties of a neural predictor. *Journal of Neurophysiology*, *96*, 2121–2126.
- Koch, G., Oliveri, M., Torriero, S., Salerno, S., Gerfo, E. L., & Caltagirone, C. (2006). Repetitive TMS of cerebellum interferes with millisecond time processing. *Experimental Brain Research*, *179*, 291–299.
- Krebs, M. O., Gut-Fayand, A., Amado, I., Daban, C., Bourdel, M. C., Poirier, M. F., et al. (2001). Impairment of predictive saccades in schizophrenia. *NeuroReport*, *12*, 465–469.
- Lawrence, B. M., & Snyder, L. H. (2006). Comparison of effector-specific signals in frontal and parietal cortices. *Journal of Neurophysiology*, *96*, 1393–1400.

- Lee, K. H., Egleston, P. N., Brown, W. H., Gregory, A. N., Barker, A. T., & Woodruff, P. W. (2007). The role of the cerebellum in subsecond time perception: Evidence from repetitive transcranial magnetic stimulation. *Journal of Cognitive Neuroscience*, *19*, 147–157.
- Linkenkaer-Hansen, K., Nikouline, V. V., Palva, J. M., & Ilmoniemi, R. J. (2001). Long-range temporal correlations and scaling behavior in human brain oscillations. *Journal of Neuroscience*, *21*, 1370–1377.
- MacDorman, C. E. (1962). Synchronization with auditory models of varying complexity. *Perceptual and Motor Skills*, *15*, 595–602.
- Matell, M. S., & Meck, W. H. (2004). Cortico-striatal circuits and interval timing: Coincidence detection of oscillatory processes. *Cognitive Brain Research*, *21*, 139–170.
- Mates, J. (1994a). A model of synchronization of motor acts to a stimulus sequence. I. Timing and error corrections. *Biological Cybernetics*, *70*, 463–473.
- Mates, J. (1994b). A model of synchronization of motor acts to a stimulus sequence. II. Stability analysis, error estimation and simulations. *Biological Cybernetics*, *70*, 475–484.
- Mates, J., Radil, T., Müller, U., & Pöppel, E. (1994). Temporal integration in sensorimotor synchronization. *Journal of Cognitive Neuroscience*, *6*, 332–340.
- Mauk, M. D., & Buonomano, D. V. (2004). The neural basis of temporal processing. *Annual Review of Neuroscience*, *27*, 307–340.
- Meck, W. H., & Benson, A. M. (2002). Dissecting the brain's internal clock: How frontal-striatal circuitry keeps time and shifts attention. *Brain and Cognition*, *48*, 195–211.
- Meck, W. H., Church, R. M., Wenk, G. L., & Olton, D. S. (1987). Nucleus basalis magnocellularis and medial septal area lesions differentially impair temporal memory. *Journal of Neuroscience*, *7*, 3505–3511.
- Medina, J. F., Carey, M. R., & Lisberger, S. G. (2005). The representation of time for motor learning. *Neuron*, *45*, 157–167.
- Michon, J.A. (1967). Timing in temporal tracking. Soesterberg, The Netherlands: Institute for Perception RVO-TNO.
- Miyake, Y., Onishi, Y., & Poppel, E. (2004). Two types of anticipation in synchronization tapping. *Acta Neurobiologiae Experimentalis*, *64*, 415–426.
- Paré, M., & Hanes, D. P. (2003). Controlled movement processing: Superior colliculus activity associated with countermanded saccades. *Journal of Neuroscience*, *23*, 6480–6489.
- Peng, C.-K., Havlin, S., Stanley, H. E., & Goldberger, A. L. (1995). Quantification of scaling exponents and crossover phenomena in nonstationary heartbeat time series. *Chaos*, *5*, 82–87.
- Rao, S. M., Harrington, D. L., Haaland, K. Y., Bobholz, J. A., Cox, R. W., & Binder, J. R. (1997). Distributed neural systems underlying the timing of movements. *Journal of Neuroscience*, *17*, 5528–5535.
- Reddi, B. A., & Carpenter, R. H. (2000). The influence of urgency on decision time. *Nature Neuroscience*, *3*, 827–830.
- Ron, S., Schmid, R., & Orpaz, D. (1989). Applying a model of saccadic prediction to patients' saccadic eye movements. *Brain Behavior and Evolution*, *33*, 179–182.
- Ross, S. M., & Ross, L. E. (1987). Children's and adults' predictive saccades to square wave targets. *Vision Research*, *27*, 2177–2180.
- Savitzky, A., & Golay, M. J. E. (1964). Smoothing and differentiation of data by simplified least squares procedures. *Analytical Chemistry*, *38*, 1627–1639.
- Schlerf, J. E., Verstynen, T. D., & Ivry, R. B. (2006). fMRI measurements of the cerebellar response to nonrhythmic movements. Program no. 653.17. *2006 Neuroscience Meeting Planner*. Atlanta, GA: Society for Neuroscience (Abstract).
- Schmid, R., & Ron, S. (1986). A model of eye tracking periodic square wave target motion. *Biological Cybernetics*, *54*, 179–188.
- Schöner, G. (2002). Timing, clocks, and dynamical systems. *Brain and Cognition*, *48*, 31–51.
- Schöner, G., Haken, H., & Kelso, J. A. (1986). A stochastic theory of phase transitions in human hand movement. *Biological Cybernetics*, *53*, 247–257.
- Schulze, H.-H. (1992). The error correction model for the tracking of a random metronome: Statistical properties and an empirical test. In F. Macar & W. J. Friedman (Eds.), *Time, action and cognition. Towards bridging the gap* (vol. 66, pp. 275–286). Dordrecht: Kluwer.
- Shelhamer, M. (2005). Sequences of predictive saccades are correlated over a span of ~2 s and produce a fractal time series. *Journal of Neurophysiology*, *93*, 2002–2011.
- Shelhamer, M., & Joiner, W. M. (2003). Saccades exhibit abrupt transition between reactive and predictive; predictive saccade sequences have long-term correlations. *Journal of Neurophysiology*, *90*, 2763–2769.
- Sigman, M., & Dehaene, S. (2005). Parsing a cognitive task: A characterization of the mind's bottleneck. *PLoS Biology*, *3*, 334–349.
- Simó, L. S., Krisky, C. M., & Sweeney, J. A. (2005). Functional neuroanatomy of anticipatory behavior: Dissociation between sensory-driven and memory-driven systems. *Cerebral Cortex*, *15*, 1982–1991.
- Stark, L., Vossius, G., & Young, L. R. (1962). Predictive control of eye tracking movements. *IRE Transactions on Human Factors and Electronics HFE*, *3*, 52–57.
- Tian, J. R., Zee, D. S., Lasker, A. G., & Folstein, S. E. (1991). Saccades in Huntington's disease: Predictive tracking and interaction between release of fixation and initiation of saccades. *Neurology*, *41*, 875–881.
- Treisman, M. (1963). Temporal discrimination and the indifference interval. Implications for a model of the "internal clock". *Psychology Monographs* *77*, 1–31.
- Ventre, J., Zee, D. S., Papageorgiou, J., & Reich, S. (1992). Abnormalities of predictive saccades in Hemi-Parkinson's disease. *Brain*, *115*, 147–165.
- Vorberg, D., & Wing, A. (1996). Modelling variability and dependence in timing. In H. Heuer & S. W. Keele (Eds.), *Handbook of perception and action* (vol. 2, pp. 181–262). San Diego, CA: Academic.
- Vos, P. G., & Hlsper, E. L. (1992). Tracking simple rhythms: On-beat versus off-beat performance. In F. Macar & W. J. Friedman (Eds.), *Time, action and cognition. Towards bridging the gap* (vol. 66, pp. 287–299). Dordrecht: Kluwer.
- Wagenmakers, W.-J., Farrell, S., & Ratcliff, R. (2004). Estimation and interpretation of $1/f^{\alpha}$ noise in human cognition. *Psychonomic Bulletin & Review*, *11*, 579–615.
- Wing, A., Daffertshofer, A., & Pressing, J. (2004). Multiple time scales in serial production of force: A tutorial on power spectral analysis of motor variability. *Human Movement Science*, *23*, 569–590.
- Wing, A. M., Keele, S., & Margolin, D. I. (1984). Motor disorder and the timing of repetitive movements. *Annals of the New York Academy of Sciences*, *423*, 183–192.
- Wing, A. M., & Kristofferson, A. B. (1973a). Response delays and the timing of discrete motor responses. *Perception and Psychophysics*, *14*, 5–12.
- Wing, A. M., & Kristofferson, A. B. (1973b). The timing of interresponse intervals. *Perception and Psychophysics*, *13*, 455–460.
- Woodrow, H. (1930). The reproduction of temporal intervals. *Journal of Experimental Psychology*, *13*, 473–499.
- Zambarbieri, D., Schmid, R., & Ventre, J. (1987). Saccadic eye movements to predictable visual and auditory targets. In J. K. O'Regan & A. Levy-Schoen (Eds.), *Eye movements: From physiology to cognition* (pp. 131–140). North Holland: Elsevier.
- Zorn, A., Joiner, W. M., Lasker, A. G., & Shelhamer, M. (2007). Sensory versus motor information in the control of predictive saccade timing. *Experimental Brain Research*, *179*, 505–515.